



# Repair Effects of Depakene on Neuropathological Changes in Cuprizone Model of Demyelination

Somayeh Sohaili<sup>1</sup>, Ardeshir Moayeri<sup>1</sup>, Marzieh Darvishi<sup>1\*</sup>, Naser Abbasi<sup>2,3</sup>

<sup>1</sup> Department of Anatomy, Faculty of Medicine, Ilam University of Medical Sciences, Ilam, Iran.

<sup>2</sup> Biotechnology and Medicinal Plants Research Center, Ilam University of Medical Sciences, Ilam, Iran.

<sup>3</sup> Department of Pharmacology, Medical School, Ilam University of Medical Sciences, Ilam, Iran.

## ABSTRACT

**Introduction:** Epigenetic advances have led to the production of a specific class of medicines called epigenetic drugs, medications that inhibit histone deacetylase (HDACi). Valproic acid (VPA), known as HDACi, has neuroprotective effects. The current study investigated the histological and functional changes of a demyelination model associated with VPA treatment in C57BL/6 mice. **Material & method:** In the present study, 48 C57BL/6 mice were classified randomly into eight groups: sham, cuprizone (0.2%), three VPA groups (treated with 100, 200, and 300 mg/kg of VPA), three groups of cuprizone plus VPA (100, 200, and 300 mg/kg of VPA). One week after treatment, gliosis, apoptosis, and remyelination were examined histologically, and locomotor function was assessed by the behavioral test. **Result:** The expression of GFAP and caspase-3 in the untreated controls had the highest immunofluorescence, while it was significantly decreased in the VPA groups ( $P < 0.05$ ). The lowest expression of these two markers was observed in the 200 mg/kg VPA group, which also had the highest expression of MBP. Behavioral tests showed that mice in the 200 mg/kg VPA group achieved the highest score and the results of the histological examination were consistent with the results of the behavioral test. **Conclusion:** The data demonstrated that there was an improvement of the demyelination models of mice treated with an optimal dose of VPA, characterized by an increase in remyelination and an increase in the behavioral score.

**Key Words:** Glial scar, demyelination models, inflammation, valproic acid (VPA), HDAC inhibitor.

eIJPPR 2020; 10(5):256-269

**HOW TO CITE THIS ARTICLE:** Somayeh Sohaili, Ardeshir Moayeri, Marzieh Darvishi, Naser Abbasi (2020). "Repair Effects of Depakene on Neuropathological Changes in Cuprizone Model of Demyelination", International Journal of Pharmaceutical and Phytopharmacological Research, 10(5), pp.256-269.

## INTRODUCTION

Multiple sclerosis (MS) is an inflammatory demyelinating illness that is described by multifocal lesions to CNS myelin. [1, 2] Despite the fact that the etiology of MS has yet to be identified, likely risk factors to its development are both genetic and environmental. [3, 4] The disease results in proinflammatory Th1 cytokine secretion and thereby leads to the destruction of the myelin sheaths that surround axons and the recruitment of other T cells and monocytes. Activated T cells generate inflammatory cytokines (interferon- $\gamma$  (IFN- $\gamma$ ), interleukin (IL)-4, and IL-17), and tumor necrosis factor  $\alpha$  (TNF $\alpha$ ). [5, 6] These inflammatory cytokines and chemokines with fenestration of the blood-brain barrier (BBB) may result in the oligodendrocyte death, demyelination, axonal damage, and gliosis. [7, 8]

Axonal damage results in an increase in the disability and symptoms of MS, including weakness, ataxia, fatigue, spasticity, cognitive deficits, depression, and pain. [9, 10] Experimental demyelination, the most typically used animal model for MS, can be induced in species by several toxins such as cuprizone and ethidium bromide. [11, 12] By inhibiting copper-dependent mitochondrial enzymes, cuprizone induces demyelination in various regions of CNS. [13] This destructive mechanism in the cell respiratory chain causes oligodendrocyte damage that leads to consistent demyelination. [13, 14] Other histopathological findings are astrocyte, microglia, and macrophage accumulation in the affected region. Those cell types play a pivotal role in cytokine release and inflammation mediated by self-reactive immune responses. [15, 16] TNF promotes proliferation of adult human and

**Corresponding author:** Marzieh Darvishi

**Address:** Department of Anatomy, Faculty of Medicine, Ilam University of Medical Sciences, Ilam, Iran.

**E-mail:** ☒ Darvish-m@medilam.ac.ir

**Relevant conflicts of interest/financial disclosures:** The authors declare that the research was conducted in the absence of any commercial or financial relationships that could be construed as a potential conflict of interest.

**Received:** 10 July 2020; **Revised:** 24 October 2020; **Accepted:** 26 October 2020



neonatal astrocytes such that cytokines can result in glial scar formation. Glial scarring prevents neurogenesis, axonal regeneration, and vascularization. Besides, there is a relationship between the expression of apoptosis-associated protein and the occurrence of lesions. [17-20]

Anti-inflammatory and anti-apoptotic agents for treatment have been revealed to improve the outcome of MS. Previous investigations demonstrated an anti-inflammatory impact with valproic acid (VPA; 2-propyl-pentanoic acid), a histone deacetylase inhibitor (HDACi), improves behavioral movement, astrogliosis and axonal loss in female rats. [21, 22] VPA is an epigenetic modulator for modifying chromatin structure and decreasing the expression of inflammatory cytokines, which reduces gliosis. [23] VPA has been revealed to manage differentiation and proliferation of neurons by promoting neurotrophin expression. [24] Some investigations have focused on the protective influence of VPA on neural cells by increasing the expression of anti-apoptotic gene and oxidative stress. [25, 26] In the present research, we assessed the impact of reducing gliosis levels by utilization of VPA on sensory motor activity, remyelination, and neurogenesis as well as on apoptosis and inflammation in cuprizone-treated animals.

## MATERIALS AND METHODS

### Mice strain and demyelination (cuprizone administration)

All experiments were performed on male mice aged 8 to 9 weeks belonging to the C57BL/6 strain (Pasteur Institute, Tehran, Iran) weighing 19-21 grams. They were kept on a 12-hour light/dark cycle at room temperature ( $22\pm 0.5$  °C) with standard mouse food and water *ad libitum*. All protocols were performed in accordance with the guidelines of the Ethical Committee of the Faculty of Medical Sciences at the Ilam University of Medical Sciences. In order to generate a demyelination model, the animals were fed a diet containing 0.2% cuprizone mixed into ground standard rodent chow for five weeks. Control groups used normal rodent chow.

### Experimental Design

In the *in vitro* study, 48 animals were divided randomly into eight groups: group 1 was the sham group that fed regular Global Rodent Chow for 5 weeks with intra-peritoneal (i.p.) injection of normal saline (NS) for the last three days (positive control: PC); group 2 was the cuprizone group that received rodent chow mixed with 0.2% cuprizone for five weeks and received i.p. injection of NS for the last 3 days (or negative control: NC); groups 3, 4, and 5 received cuprizone plus VPA (treated with 100, 200 and 300 mg/kg (i.p.) during the last 3 days of 5-week cuprizone feeding, respectively); groups 6, 7, and 8 consisted of healthy mice that received three doses of VPA (100, 200 and 300 mg/kg)

separately for 3 days. Six male mice were used in each experimental group. [27]

### Determine body weight

The measurement of body weight was performed over six weeks from the start of the treatment protocol. In order to compare body weights in different groups, animals were weighed every week and findings are shown as the mean and standard deviation. The assessment of mean values was carried out by one-way analysis of variance (ANOVA).

### Motor tasks assessments

#### • Clinical assessment

Neuromuscular severity scores were obtained once per week in the sham, Cup, Cup plus VPA, and healthy VPA groups during the six weeks of the experiment. The clinical signs of weakness were monitored using a published 6-point scale according to the following standard: 0 = normal strength and tone without any symptoms; 1 = loss of tail tone with mild weakness; 2 = moderate hind limb weakness (weakness of one hind limb); 3 = severe hind limb weakness (paralysis of both hind limbs); 4 = severe forelimb weakness (paralysis of both forelimbs); 5 = pre-morbid state; 6 = death. Intermediate scores were considered for asymmetrical weakness. [28]

#### • Balance beam test

In addition, the ability of the animals to maintain balance was investigated as reported in Boltze et al. [29] Mice were evaluated by a balance beam test that is part of the Modified Neurological Severity Scale (MNSS) and consists of a 6-point scale that includes posture balances (0), catches of beam (1), one limb falls down from the beam and hugs the beam (2), two limbs fall and hug the beam in more than 60s (3), tries to balance but falls off in more than 40s (4), attempts to balance but falls off in more than 20s (5), and no attempt to balance and falls off (6).

#### • Footprint test

A footprint test was performed to compare the gait of cuprizone mice with that of VPA, Cup plus VPA, and sham groups. To determine footprints, the hind and fore paws of the mice were marked with black and blue non-toxic paints, respectively. Then, the mice walked across a 50 cm long platform, with walls of 10 cm width and 10 cm height. The footprint patterns (cm) were measured and analyzed for four-step parameters (Figure 1).

- Stride length (ST): the average distance between each stride.
- Hind-base width (HBW): the average distance between the left and right hind footprints.
- Front-base width (FBW): the average distance between the left and right front footprints.
- Overlap of front and hind footprint (OV).

The values were recorded from each run and the average value of each set was used in the subsequent analysis. [30]

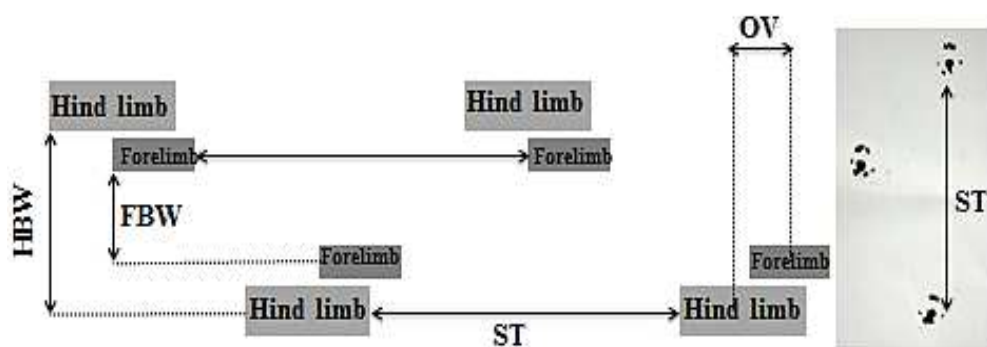


**Figure 1.** Schematic representation of footprint parameters (stride length (ST), Hind-base width (HBW), Front-base width (FBW), Overlap of front and hind footprint (OV)).

- **Passive avoidance test (PAT)**

A shuttle box test was carried out to assess the learning memory of the mice. The apparatus included a light and a dark chamber which were connected by a guillotine door. The floor of the device had a stillness grid with a separate stimulator for the generation of electrical shock. The PAT was assessed for two subsequent days. The first day included two stages of habituation and training. In the initial habituation, the animal was put in the illuminated chamber and after 20 seconds the dividing door was opened and the mice, based on the natural instinct, moved into the darkened area. Then, the door was closed and after 30 seconds the mice were returned to the home cage. The second habituation was repeated 30 minutes after the initial habituation. Then, the training was conducted 30 minutes after secondary habituation. For training, the mice were placed in the illuminated area and after the mice entered the darkened chamber, the door was closed and a foot shock (0.4 mA for 1.5 sec) was initiated. After 20 seconds, the mice were returned to the home cage. After 2 minutes, the previous step was repeated. If the latency to enter the dark chamber was < 120 sec, the training step was repeated. On the second day, the evaluation of short term learning, the latency to cross the door (Step Through Latency=STL) and remain in the darkened area (Time spent in Dark Compartment =TDC) were measured without electrical shock. [31]

### **Histological assessment**

Mice were anesthetized with ketamine (50 mg/kg) and xylazine (4 mg/kg) and then the left heart ventricle was perfused with phosphate-buffered saline (PBS) followed by 4% paraformaldehyde. Brains were removed, fixed overnight in 4% paraformaldehyde, and embedded in paraffin. Subsequently, the coronal section was used for evaluation of demyelination and remyelination, as well as apoptosis and gliosis.

- **Luxol fast blue (LFB) staining**

After hydration, the paraffin sections were incubated with 0.1 % LFB solution at 60 °C for 12 hours. The sections were transferred to 95, 70, and 50% ethanol for 10 minutes and then rinsed with water. The slides were transferred for the second time to lithium carbonate solution, 70% ethyl alcohol, and distilled water, respectively. After LFB staining, the sections were counterstained with 0.1% Cresyl fast violet for 10 s, rinsed with distilled water, dehydrated in a series of alcohols, cleared in xylene, mounted on gelatin-coated slides, and allowed to dry overnight. The corpus callosum was demonstrated by a light microscope and photographed with a camera linked to a microscope. For the investigation of demyelination, a percentage of the volume fraction was determined by dividing the damaged tissue of each section to the total area of the brain using ImageJ1.43U (NIH, USA) software. [27]

- **Immunohistochemical staining**

Immunostaining of the tissue was done to evaluate the demyelination, gliosis, and apoptosis. The slides were deparaffinized and rehydrated, permeated in PBS (10 min) with triton x-100 (0.3%) for 15 min (Sigma-Aldrich, Steinheim, Germany), and blocked in 1% FBS in PBS for 30 minutes. The endogenous peroxidase activity was inhibited by 3.0% hydrogen peroxide in PBS for 15 min. The slides were labeled overnight with primary antibodies including rabbit anti-MBP polyclonal antibody (1:300; Abcam, Cambridge, UK), anti-Caspase-3 antibody (1:500 Abcam) and mouse anti-GFAP monoclonal antibody (1: 500; Abcam, Cambridge, UK) at 4 °C, washed twice with PBS (5 min), and incubated with rabbit anti-mouse polyclonal secondary antibody conjugated with fluorescein isothiocyanate (FITC -1:100; Abcam, Cambridge, UK) or goat anti-rabbit secondary antibody conjugated with Alexa-Red (1:100; Abcam, Cambridge, UK) for 45 min. The excess secondary antibody was rinsed with PBS and the

nuclei of the cells were counterstained by 4, 6-diamidino-2-phenylindole dihydrochloride (DAPI, molecular probes, 1:10000). The sections were examined at 10x magnifications under a fluorescent microscope (Kern, Germany). The fluorescent intensity was determined utilizing the Image J software (Aherne and Dunnill).

The findings are displayed as means ± SEM. Statistical analysis was performed using one-way analysis or two-way analysis of variance (ANOVA). P-values of less than 0.05 were considered statistically significant.

## RESULT

### VPA Increased Cuprizone-Induced Weight Loss

The mean weight of the mice in the positive control group, healthy groups injected with VPA (100, 200, and 300 mg/kg dose of VPA) and the negative control (cuprizone only = Cup-group) was compared with mice received Cup plus VPA (100, 200, and 300 mg/kg) after each week of treatment. The weight of mice in the negative control and the Cup plus VPA (100, 200, and 300 mg/kg) was significantly different between the second (start time of Cup treatment) and sixth week (start of VPA treatment), while there was no significant difference between the positive control group and VPA groups. The weight of mice in the sixth week in the Cup plus VPA after VPA injection had a small increase and the weight of the negative control had a decrease from the positive control group (Table 1).

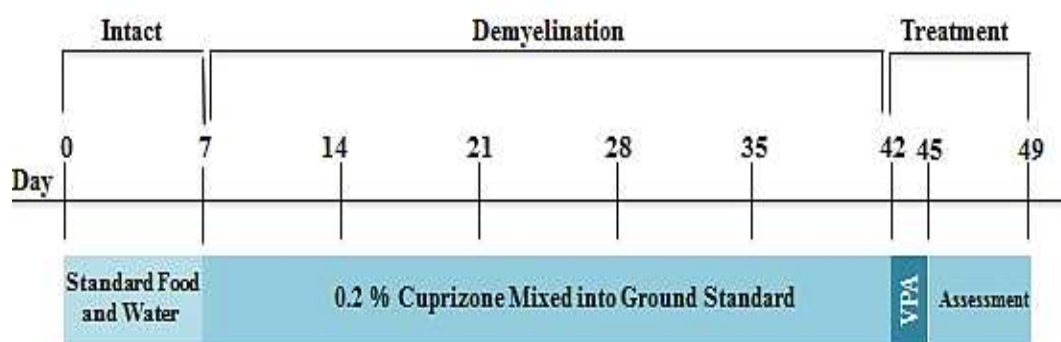


Figure 2. Time schedule of the experimental protocol.

Table 1. Average weight in mice during the treatment period (6 weeks).

Groups	7 Days	2 Weeks	3 Weeks	4 Weeks	5 Weeks	6 Weeks	7 Weeks
Control	25.5±6.5	25.5±6.5	25.75±6.5	25.5±6.5	25.5±6.5	26.25±6.7	*26±6.6
Cup	25±0.7	25±0.7	26.25±0.8	26±0.4	26.25±0.4	*24.75±1.9	*24.5±2.1
Cup+VPA300	24.5±0.6	24.5±0.6	24.25±0.25	25.75±0.4	25.125±0.8	*24.5±0.9	*26.5±0.6
Cup+VPA200	26.5±0.2	25.5±0.64	24.25±1.7	26.5±0.6	26.625±0.6	*25.25±1.4	*27.375±0.5
Cup+VPA100	25.5±0.6	25±0.95	24.5±0.9	25.25±0.8	25.75±0.4	*24.75±0.4	*27±1.08
VPA300	25±0.25	25±0.25	25.75±0.25	25.75±0.25	26.25±0.25	26.25±0.25	*26.5±0.28
VPA200	25.5±0.28	25.5±0.28	25.75±0.28	25.5±0.28	25.5±0.28	26.25±0.25	*26.25±0.25
VPA100	25.75±0.4	25.75±0.4	26.25±0.25	26±0.4	26±0.4	26.75±0.4	*26.5±0.28

Results are shown as mean ± SEM and analyzed by one-way ANOVA. Asterisks indicate significant differences between the positive control and other groups (\*P<.05, with Bonferroni's correction for multiple comparisons).

### Clinical assessment

The mice of the Cup-group were presented with a moderate weakness that progressed to severe hind- and fore-limb weakness (associated with significant weight loss). This score gradually increased with age. In the Cup plus VPA

groups, the results showed a decrease and then an increase in neuromuscular severity scores. The analysis demonstrated that the lowest score of the clinical test was at 200 mg/kg of VPA, which was significantly lower than those scores at the other doses of VPA used in the study (mean± SEM neuromuscular severity scores of 2±0.4 at five weeks, *p* = 0.002). The positive control and VPA groups showed no significant differences in clinical tests at five weeks of follow up.

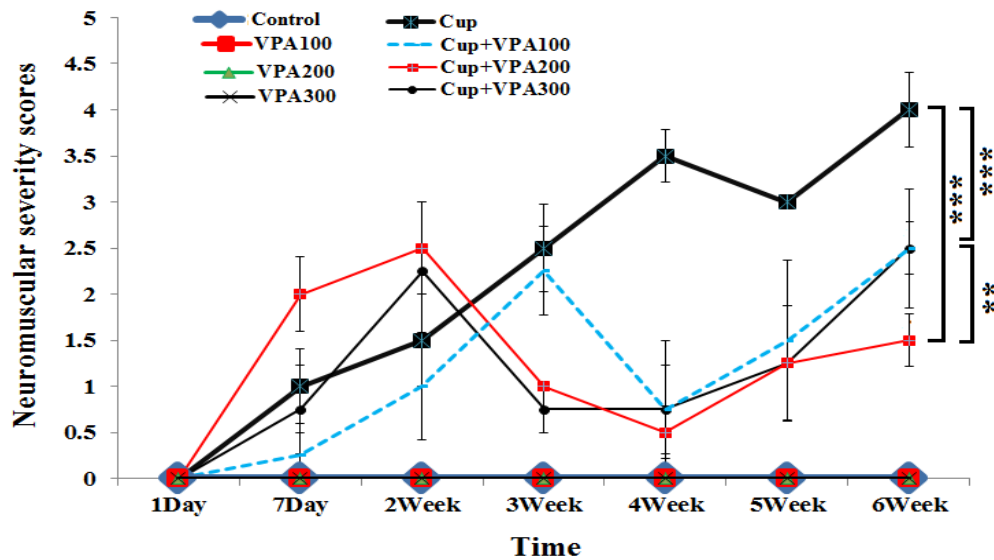


Figure 3. Neuromuscular severity score. This figure shows the mean neuromuscular severity scores of the Cup and Cup plus VPA male mice. There is a progressive weakness in Cup mice (black lines) from weeks 1 to 6 of the experiment. There is a progression in weakness in Cup plus VPA (100, 200, and 300 mg/kg) from weeks 1 to 5 and a decrease from weeks 5 to 6. Based on this score, the progression can be divided into a disease onset phase (1-14 days) and a progressive phase (2-5 weeks). \*\* indicates  $p < 0.01$  comparing Cup plus VPA with Cup mice, \*\*\* indicates  $p < 0.001$  between three different doses of Cup plus VPA.

#### Balance beam test

Experimental groups were tested for motor coordination and balance on the beam test. Errors per posture balances, catches of the beam, and one or two limbs falling down from the beam to traverse were recorded for each animal. ANOVA analysis indicated that Cup animals had higher scores (indicating worse balance) compared with Cup plus

VPA mice at 5-6 weeks ( $P < 0.01$ ). Cup mice became progressively worse compared with the positive control and VPA groups at weeks 1 to 5 ( $P < 0.001$ ). In addition, Cup plus VPA animals with 200 mg/kg dose had lower scores compared with their performance at other doses of VPA ( $P < 0.001$ ).

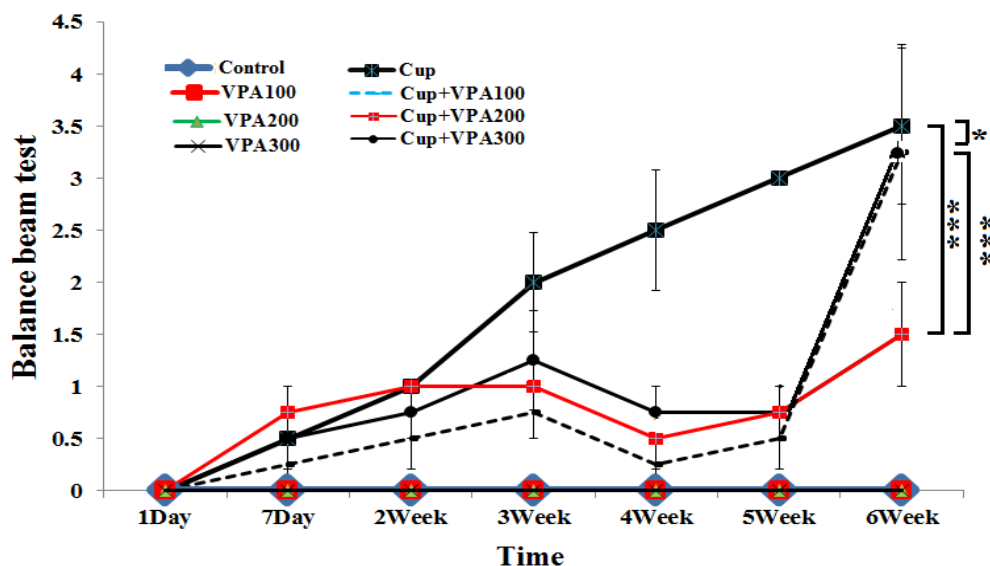


Figure 4. The balance was measured in Cup and Cup plus VPA male mice using the balance beam test (0= normal and 6= maximum). Cup mice had higher scores in traversing the beam compared with Cup plus VPA mice. In addition, the positive control and healthy groups injected with VPA (100, 200 and 300 mg/kg) showed no differences. Values are expressed as mean  $\pm$  SEM. \* indicates  $P < 0.05$  comparing Cup plus VPA 100 with Cup mice, \*\* indicates  $P < 0.01$  comparing Cup plus VPA300 and 200 with Cup mice, \*\*\* indicates  $p < 0.001$  between three different doses of Cup plus VPA.

### Footprint test

Errors per step were assessed by analyzing the footprints of mice while they walked along a narrow corridor. Footprint patterns of Cup and Cup plus VPA mice at weeks 1 to 6 of the experimental procedure are presented in Figure 5. At all weeks of the experiment, the positive control and VPA groups walked in a straight line with a regular gait: locating the hind paw at the position where the ipsilateral forepaw had been in the previous step. In contrast, Cup mice progressively walked from side to side, with shorter steps, vibrational and staggering movements, and unregular gait. In the Cup plus VPA group, a quantitative type of walking with 4 parameters (ST, FBW, HBW, and OV) was evaluated. The ST of the positive control and healthy groups increased significantly with age. In contrast, from weeks 1 to 6, Cup mice displayed a significantly shorter ST compared to positive control mice ( $P < 0.001$ ). In addition, the ST of Cup plus VPA mice did not differ from that of the Cup group from weeks 1 to 5, but in the last week, after treatment by VPA, the ST increased significantly relative to the Cup mice ( $P < 0.05$ ) (Figure 5A). The OV showed uniformity of step alternation. As shown in Figure 5B, Cup and Cup plus VPA mice indicated a

similar disruption in step alternation from weeks 1 to 5 experimental procedures compared with the positive control and healthy groups, but at the sixth week the regular left-right step pattern presented uniformly, and they exhibited a lesser distance between front and hind footprint pattern (a decreased overlap) compared with Cup mice. The lowest distance was for the groups that received 200 mg/kg of VPA ( $P < 0.008$ ).

The FBW of Cup mice were significantly wider than that demonstrated by the positive control and VPA groups at weeks 1 to 6 of the experiment, while in the Cup plus VPA group, the distance was high until the fifth week and decreased from 5 to 6 weeks. However, there was no difference between the treatment groups with VPA (Figure 5C). The findings showed that the HBW of Cup mice was significantly less than that presented by the positive control and VPA groups during the experiment. In the Cup plus VPA group, the distance was low until the fifth week and increased from weeks 5 to 6. The highest increase of HBW was in the group receiving the dose of 200 mg/kg VPA; this increase was significantly different with the positive control group ( $P < 0.05$ ) (Figure 5D).

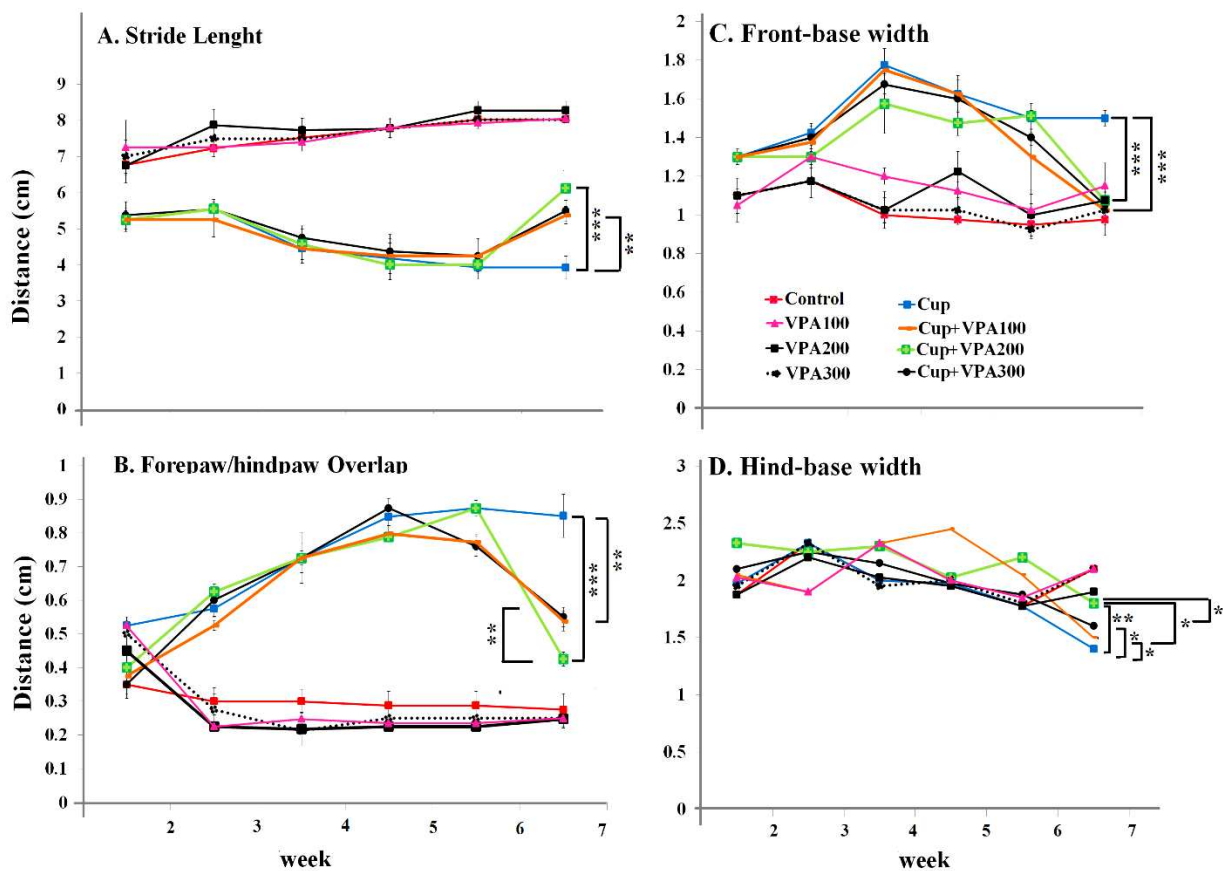


**Figure 5.** Quantitative analysis of footprint patterns in experimental groups, based on the stride length (A), the distance between the front and hind footprint overlap (B), front base width (C) and hind base width (D). Values indicate means  $\pm$  SEM by mice of each group at weeks 1 to 6 (\* $P < 0.05$ ; \*\* $P < 0.01$ ; \*\*\* $P < 0.001$ ; with Bonferonni's correction).

### Passive avoidance test (PAT)

Figures 6A and B show STL and TDC in PAT after training. The findings showed a significant difference in STL and TDC among different experimental groups. Tukey's post-hoc analysis indicated that Cup plus VPA (100, 200, and 300 mg/kg) dose-dependently increased STL and reduced TDC compared with the Cup group. These results indicate that Cup may increase impairment effects on PAL and could be investigated in the subsequent experiments.

The analysis showed significant differences in STL and TDC among the Cup and the Cup plus VPA groups ( $P > .05$ ). However, statistical analysis indicated that STL of the positive control and VPA groups in all doses was significantly greater than the Cup group ( $P < .001$ ). Besides, TDC of the positive control and VPA groups were less than Cup mice ( $P < .01$ ). Moreover, VPA across all dosages decreased the impairment effect of Cup on memory and PAL.

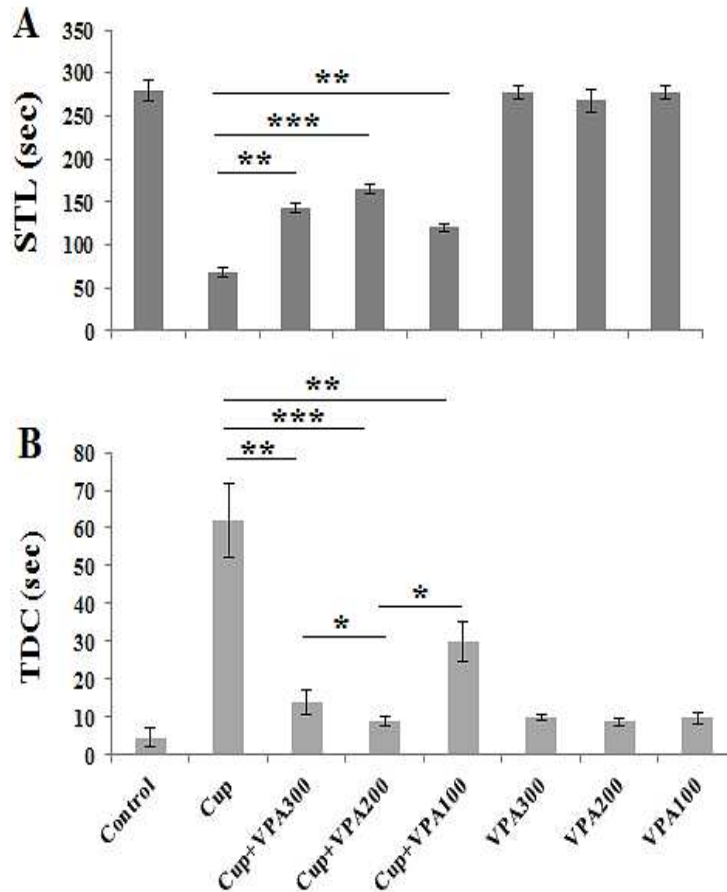
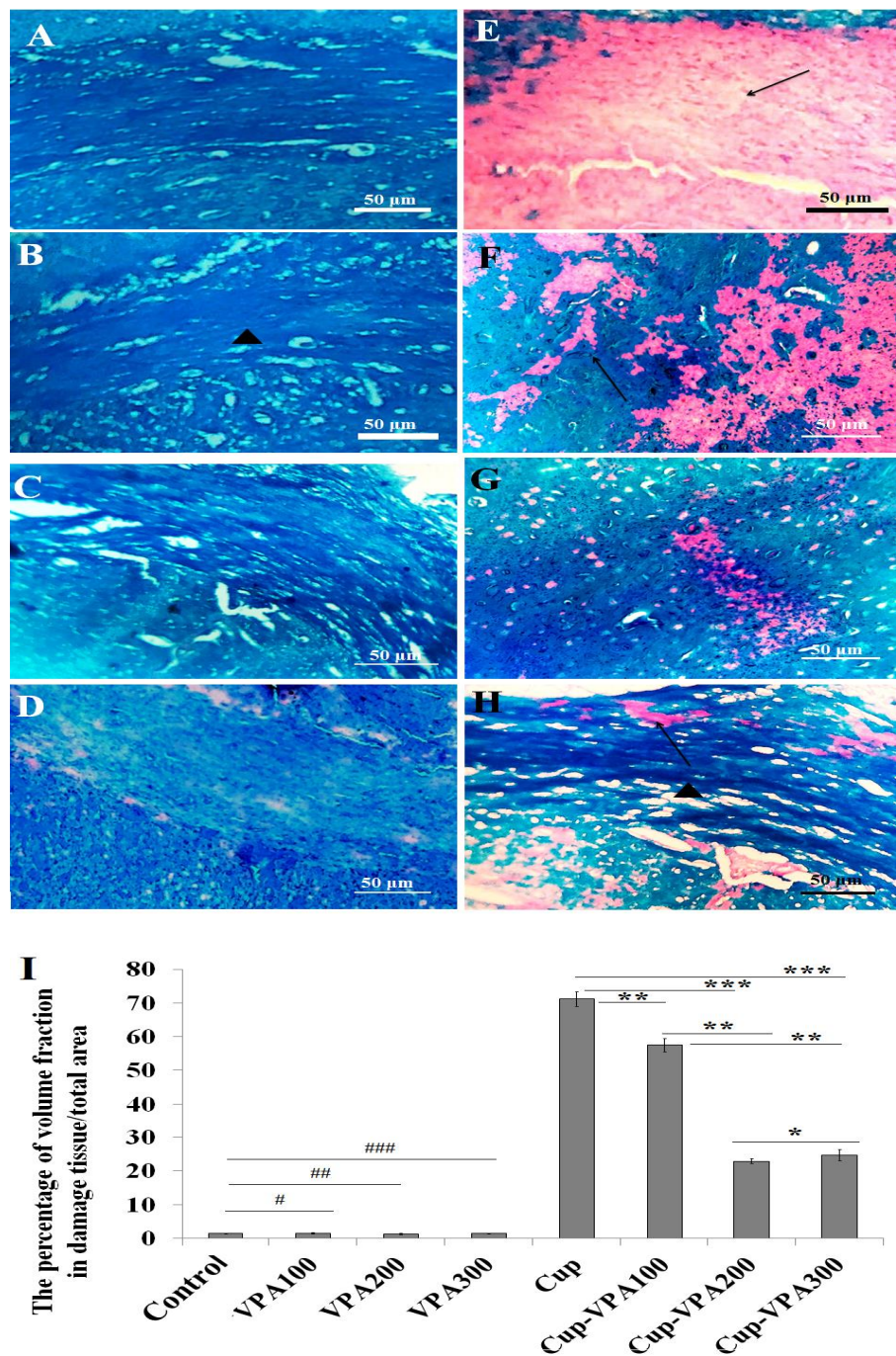


Figure 6. Effect of saline and VPA (100, 200, and 300 mg/kg) on (A) step-through latency (STL) in the passive avoidance test (PAT) and (B) Time spent in the dark compartment (TDC) in the PAT. Each symbol indicates mean  $\pm$  SEM, \* $P < .05$ , \*\* $P < .01$ , \*\*\* $P < .001$ .

### Luxol fast blue (LFB) staining

Figure 7 shows the demyelination in the positive control (A), VPA treated groups (B-D), the untreated Cup group (E), and the Cup plus VPA groups (100, 200, and 300 mg/kg). The severity of demyelination in the corpus callosum can be seen in the untreated group (E), while the

VPA at all different doses affected the myelin loss induced by cuprizone administration, and resulted in the formation of the myelin sheath and brain tissue repair. VPA significantly enhanced myelin formation compared to the Cup group (Figure 7I).



**Figure 7.** Effect of different doses of VPA (100, 200, and 300 mg/kg) on myelin sheath in cuprizone model of mice. The blue areas indicate intact regions (in experimental, positive control, and cuprizone groups) whereas the pink areas illuminate demyelinating regions. There was a statistically significant difference among Cup plus VPA in different doses (100, 200 and 300 mg/kg) and the Cup groups. The arrowhead is the myelin sheath and intact area, and the arrow indicates a demyelination region. Symbols indicate mean  $\pm$  SEM. Scale bar equals 50  $\mu$ m ( $\times 10$ ). #  $P < .14$ , ##  $P < .09$  and ###  $P < .21$ . (\* $P < .05$ , \*\* $P < .01$ , \*\*\* $P < .001$ ).

### Immunohistochemical staining

Figure 8 represents a high immunoreactivity of GFAP in the Cup group. In contrast, there was a lower reactivity in the Cup plus VPA at all different doses. The brain tissue in the Cup plus VPA groups showed lower immunostaining than in the Cup group but higher immunostaining with GFAP than those of the positive control and VPA groups.

The quantitative investigation illustrated that the lowest relative intensity was observed at 200 mg/kg. The relative intensity of the gliosis marker of GFAP in the Cup group indicates that there was more than a ten-fold increase compared with the positive control and VPA groups ( $P < 0.05$ ). Furthermore, this figure represents the high immunoreactivity of MBP in the positive control group in

contrast to the Cup group. Cuprizone significantly reduced myelin protein compared to the positive control mice. VPA at all different doses induced myelination in brain tissue. A higher relative intensity was observed at the positive control and VPA groups and in the Cup plus VPA groups with doses of 200, 300, and 100 mg/kg, respectively. Also, the lowest immunostaining with MBP was seen in the Cup group.

Caspase-3 has long been known to have an important role in the regulation of apoptosis. Our results demonstrated that a 5-week administration of cuprizone significantly

increased caspase-3 expression in Cup mice compared to the positive control and VPA groups (100, 200, and 300 mg/kg). As shown in Figures 9F-H, the expression of caspase-3 was significantly decreased in Cup plus VPA mice at all different doses compared to the Cup group. Results showed that the lowest mean percentage of positive cells was noticed at 200 mg/kg, which shows the anti-apoptotic effect of VPA at an optimum dose via suppressing caspase-3 activation. Furthermore, the injection of VPA increased caspase-3 expression in mice that only received VPA compared to the positive control mice (Figure 9B-D).

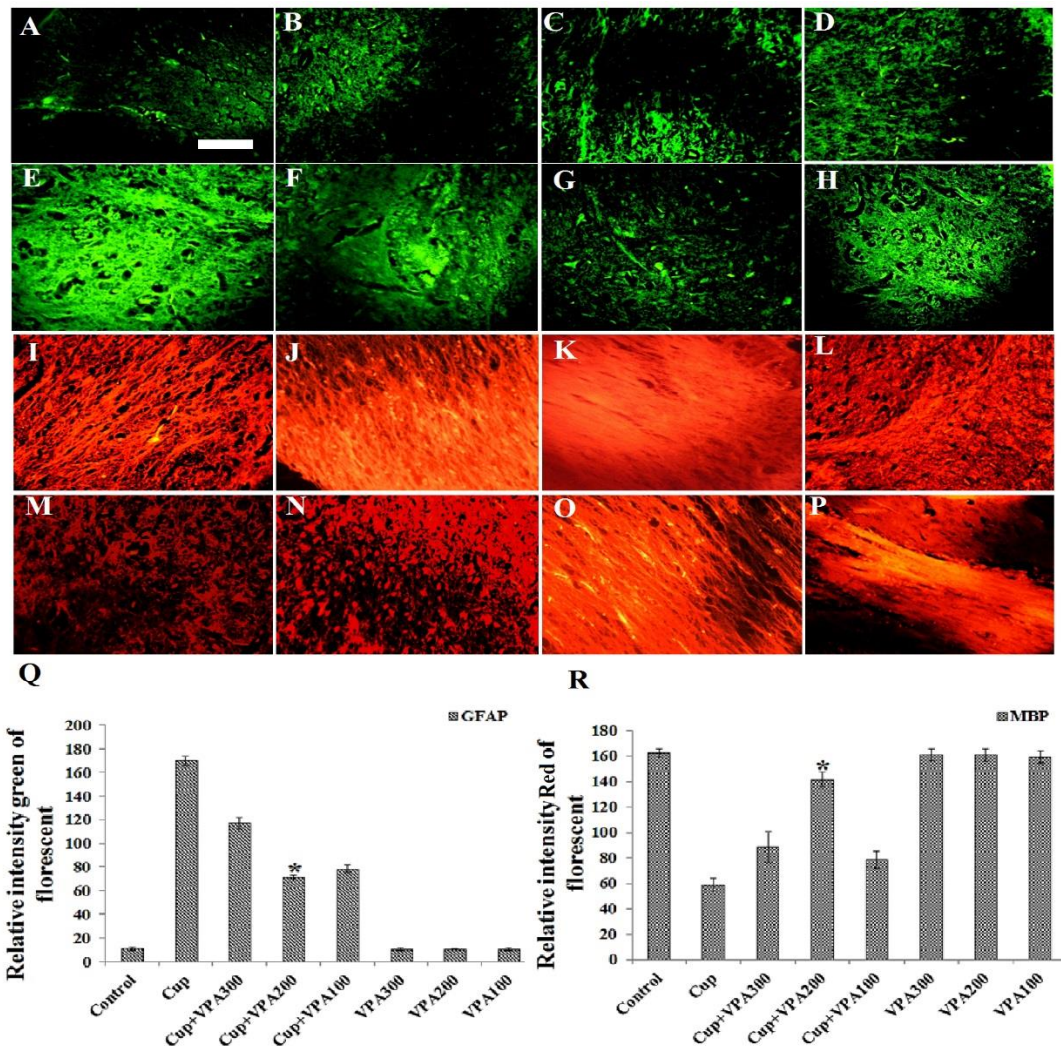


**Figure 8.** The effect of valproic acid (VPA) on glial fibril acidic protein (GFAP) and myelin basic protein (MBP) expression in brain tissue using the immunofluorescent technique (6 weeks post cuprizone demyelination). The first (A-D) and second (E-H) panels represent the GFAP expression. A-D indicate positive control and VPA (100, 200, and 300 mg/kg of VPA) groups, respectively. E-H show the Cup and Cup plus VPA (100, 200, and 300 mg/kg of VPA), respectively. The third (I-L) and fourth (M-P) panels represent MBP expression in a brain section. I-L illustrates the positive control and VPA (100, 200, and 300 mg/kg of VPA) groups, and M-P represents the Cup and Cup plus VPA (100, 200, and 300 mg/kg of VPA), respectively (scale bars = 50  $\mu$ m). Q and R show the relative intensity of immunofluorescence (gray level values) of the GFAP and MBP in demyelinated mice treated with different doses of VPA (100, 200 and 300 mg/kg). The asterisk indicates that the value of GFAP and MBP expression at the optimal dose of “200 mg/kg” is significantly different compared with those at the other doses of VPA (\* $P$ <0.05).

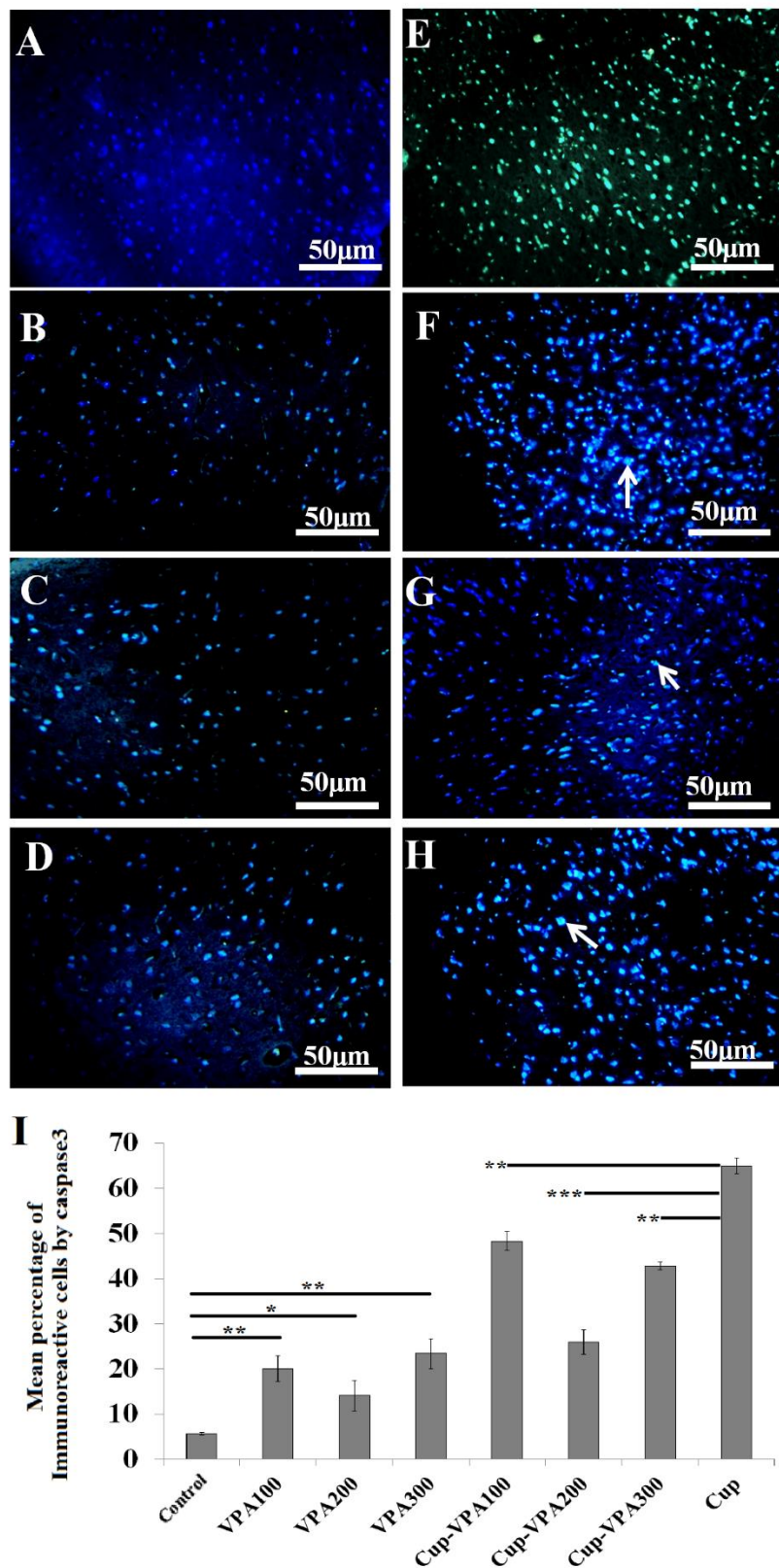


**Figure 9.** The effect of valproic acid (VPA) on caspase-3 in brain tissue using the immunofluorescent technique (6 weeks post cuprizone demyelination). The right (A-D) and left (E-H) panels show the caspase-3 expression. A-D represent the positive control and VPA (100, 200, and 300 mg/kg of VPA) groups, and E-H shows the Cup and Cup plus VPA (100, 200, and 300 mg/kg of VPA), respectively (scale bars = 50  $\mu$ m). I shows the mean percentage of immunoreactive cells by caspase-3 in experimental mice. The arrow indicates a positive cell for the expression of caspase-3 in brain tissue. Symbols indicate mean  $\pm$  SEM. (\* $P < .05$ , \*\* $P < .01$ , \*\*\* $P < .001$ ).

## DISCUSSION

The cuprizone model of demyelination has been used to investigate the process of remyelination and demyelination. [32] In this study, we evaluated the effect of different doses of VPA on locomotor and histopathological results in a cuprizone model of mice. Our results indicate that the application of VPA has modulatory effects on behavioral activity (motor and memory), apoptosis, gliosis, and myelination. In keeping with our results, the weight of mice decreased after receiving the cuprizone diet over a defined period (6 weeks), and this finding is in agreement with previous studies. This study showed that the weight of the mice treated with VPA increased during the last 7 days of treatment. Mice lost their body weight at 5 weeks of Cup feeding and then gained weight over the next week; these findings are in agreement with Sachs et al. (2014). [33] Learning and cognition deficits are also reported after demyelination by cuprizone. [34] In this model, we demonstrated the effect of VPA on memory. The effect was evaluated by a passive avoidance task measuring of STL and TDC in mice. Results showed that mice treated with VPA showed improved memory (with an increase of STL and decline of TDC). Cup plus VPA, at all different dosages, with VPA showed no significant effect on STL, TDC, or the learning capability of mice. Our results are consistent with other studies that reported HDACi upregulates memory, learning, and cognition by inducing histone H3 and H4 acetylation of brain-derived neurotrophic factor (BDNF) promoters. [35, 36] BDNF has a potent impact on development and proliferation, differentiation, neurogenesis, and survival of the neural cells in the adult hippocampal region. [37] In the present study, motor function in Cup mice was tested and results demonstrated that on all motor tests mice displayed a progressive deterioration in motor coordination and balance, compared with the positive control and healthy groups. Beneficial effects of VPA were observed to occur in motor functions and these effects were related to the dose of VPA. These results are comparable to some neurology studies, in which we have shown a significant reduction in neurological dysfunction in the demyelination model. Previous studies have shown a protective role for VPA in motor and sensory functions on spinal cord injury, Huntington's disease, and Parkinson's disease. Cuprizone increased axonal injury through the decrease of microglial activation. IL-6 production is coordinated by motor abnormalities in mice. In the demyelination model used in this investigation, the application of VPA decreases the demyelination region in brain tissue. This result obtained by LFB staining and is in agreement with previous studies that shows the administration of VPA after stroke improved neurological outcome. [38] HDAC inhibitors prevent oligodendrocyte differentiation and hypomyelination by activation of the Wnt signaling pathway. [39] VPA elevated

mature oligodendrocytes identified by MBP and myelinated axons. Furthermore, VPA augments white matter regeneration. [40]

In the histological assessment, the expression of glial fibrillar acidic protein (GFAP) was up-regulated after 5 weeks of cuprizone administration. The application of VPA reduced the relative intensity of immunofluorescence at the GFAP in Cup plus VPA mice. VPA reduces the traumatized spinal cord gliosis. However, gliosis prevents axon regeneration that its result is the highest axon loss. In this study, in the Cup group, GFAP immunoreactivity was the highest, while the behavioral test had the lowest score. In contrast, Cup plus VPA mice showed an increase in behavioral scores and a decrease in GFAP expression. NF- $\kappa$ B was revealed to be preferentially induced by astrocytes, and caused an increase of neuronal sparing, sprouting of spinal tract axons, promoted neuronal survival and elevated significant functional recovery in experimental autoimmune encephalomyelitis (EAE). [41, 42]

In addition, the myelin basic protein (MBP) produced by mature oligodendrocytes is decreased after treatment by cuprizone. Besides, treating mice with VPA resulted in the upregulation of MBP expression in the last 7 days after demyelination. This finding agrees with a recent study. [27, 30]

Extracellular glutamate caused the death of oligodendrocytes by inducing the AMPA/kainate receptor in these cells. GLT-1, as a glutamate transporter, reduces glutamate in the extracellular area and thus declines the damage to the grey and white matter brain tissue. HDAC inhibitors downregulate glutamate through the increase of GLT-1 and thus reduce oligodendrocyte death. [38] Moreover, VPA acts on white matter repair and neurogenesis through regulation of NMDA signaling, elevated BDNF, and acetylated histone H4, GABA gene expression, all of which could affect this process. [24-26]

Apoptosis has recently been revealed to occur in association with decreased reduced histone acetylation or activated E2F1 transcription factor. E2F1-induced apoptosis is performed via caspase-3. Besides, caspase-3 is activated in demyelination models of cuprizone and is associated with a reduction in motor and sensory functions and permanent disability. [43] In Cup mice treated with VPA, we showed that the caspase-3 expression component resulted in reduced brain tissue. This data is in line with investigations on the spinal cord that demonstrate downregulation of caspase-3 activation via HDAC inhibitors. Furthermore, VPA and other HDACi induce apoptosis of the microglia by inducing a loss of microglial mitochondrial transmembrane potential and promote histone hyperacetylation. A recent investigation explained VPA involvement in neuroprotective genes such as Hsp70 and Bcl-2. [44, 45]

## CONCLUSION

In the present study, we sought to establish whether HDACs could have a histological and behavioral effect on Multiple Sclerosis (MS) models. We demonstrated that VPA has a potential role for regulation of apoptosis, gliosis, and demyelination using a cuprizone model of mice. In this MS model, we showed that VPA decreased caspase-3 and GFAP activation. In addition, VPA increased the level of MBP and remyelination, which is enhanced by results of behavioral data such as PAT, footprint, and balance tests. Our findings showed that VPA may provide effective therapeutic interventions for demyelinating disease.

## REFERENCES

- [1] Popescu B, Pirko I, Lucchinetti C. Pathology of Multiple Sclerosis: Where Do We Stand? Continuum (Minneapolis, Minn). 2013; 19(4): 901–921.
- [2] Love S. Demyelinating diseases. J Clin Pathol. 2006; 59(11): 1151–1159.
- [3] Handel AE, Handunnetthi L, Giovannoni G, Ebers GC, Ramagopalan SV. Genetic and environmental factors and the distribution of multiple sclerosis in Europe. Eur J Neurol. 2010; 17(9): 1210-1214.
- [4] Abolfazli R, Samadzadeh S, Sabokbar T, Siroos B, Armaki SA, Aslanbeiki B, Ghelman M, Taheri T, Shakoori A. Relationship between HLA-DRB1\* 11/15 genotype and susceptibility to multiple sclerosis in Iran. J Neurol Sci. 2014; 345(1-2): 92-96.
- [5] Amedei A, Prisco D, Elios M. Multiple Sclerosis: The Role of Cytokines in Pathogenesis and in Therapies. Int J Mol Sci. 2012; 13(10): 13438-13460.
- [6] Singh BL, Schwartz JA, Sandrock C, Bellemore SM, Nikoopour E. Modulation of autoimmune diseases by interleukin (IL)-17 producing regulatory T helper (Th17) cells. Indian J Med Res. 2013; 138(5): 591-594.
- [7] Kiguchi N, Kobayashi Y, Kishioka S. Chemokines and cytokines in neuroinflammation leading to neuropathic pain. Curr Opin Pharmacol. 2012; 12(1): 55-61.
- [8] Kwon EE1, Prineas JW. Blood-brain barrier abnormalities in longstanding multiple sclerosis lesions. An immunohistochemical study. J Neuropathol Exp Neurol. 1994; 53(6): 625-636.
- [9] Leone C, Severijns D, Doležalová V, Baert I, Dalgas U, Romberg A, Bethoux F, Gebara B, Santoyo Medina C, Maamâgi H, Rasova K, Maertens de Noordhout B, Knuts K, Skjerbaek A, Jensen E, Wagner JM, Feys P. Prevalence of Walking-Related Motor Fatigue in Persons with Multiple Sclerosis:

- Decline in Walking Distance Induced by the 6-Minute Walk Test. Neurorehabil Neural Repair. 2016; 30(4): 373-383.
- [10] Schiavolin S, Leonardi M, Giovannetti AM, Antozzi C, Brambilla L, Confalonieri P, Mantegazza R, Raggi A. Factors related to difficulties with employment in patients with multiple sclerosis: a review of 2002-2011 literature. Int J Rehabil Res. 2013; 36(2): 105-111.
  - [11] Lassmann H, Bradl M. Multiple sclerosis: experimental models and reality. Acta Neuropathol. 2017; 133(2): 223–244.
  - [12] Pachner AR. Experimental models of multiple sclerosis. Curr Opin Neurol. 2011; 24(3): 291-299.
  - [13] Tarabozetti A, Walker T, Avila R, Huang H, Caporoso J, Manandhar E, Leeper TC, Modarelli DA, Medicetty S, Shriver LP. Cuprizone Intoxication Induces Cell Intrinsic Alterations in Oligodendrocyte Metabolism Independent of Copper Chelation. Biochemistry. 2017; 56(10): 1518–1528.
  - [14] Ghaiad H, Nooh M, El-Sawalhi M, Shaheen A. Resveratrol Promotes Remyelination in Cuprizone Model of Multiple Sclerosis: Biochemical and Histological Study. Molecular Neurobiology 2017; 54 (5): 3219–3229.
  - [15] Kollias G, Douni E, Kassiotis G, Kontoyiannis D. The function of tumour necrosis factor and receptors in models of multi-organ inflammation, rheumatoid arthritis, multiple sclerosis and inflammatory bowel disease. Ann Rheum Dis. 1999; 58: (Suppl I) I32–I39.
  - [16] Viglietta V, Baecher-Allan C, Weiner H, Hafler D. Loss of Functional Suppression by CD4+CD25+ Regulatory T Cells in Patients with Multiple Sclerosis. Jem Home. 2004; 199 (7): 971-979.
  - [17] Pekny M, Nilsson M. Astrocyte activation and reactive gliosis. Glia, 2005; 50(2005): 427-434.
  - [18] Colangelo AM, Alberghina L, Papa M. Astroglial gliosis as a therapeutic target for neurodegenerative diseases. Neuroscience Letters. 2004; 565(2014): 59–64.
  - [19] Sofroniew M. Molecular dissection of reactive astroglial gliosis and glial scar formation. Trends in Neurosciences. 2009; 32(12): 638-647.
  - [20] Fitch M, Doller C, Combs CK, Landreth G, Silver J. Cellular and Molecular Mechanisms of Glial Scarring and Progressive Cavitation: In Vivo and In Vitro Analysis of Inflammation-Induced Secondary Injury after CNS Trauma. Journal of Neuroscience. 1999; 19(19): 8182-8198.
  - [21] Xuan A, Long D, Li J, Ji W, Hong L, Zhang M, Zhang W. Neuroprotective effects of valproic acid

- following transient global ischemia in rats. *Life Sciences*, 2012; 90(11–12): 463-468.
- [22] Kassis H, Chopp M, Liu X, Shehadah A, Roberts C, Zhang ZG. Histone deacetylase expression in white matter oligodendrocytes after stroke. *Neurochemistry International*, 2014; 77(2014): 17-23.
- [23] Ximenes JC, Goncalves D, Siqueira RM, Neves KR, Santos Cerqueira G, Correia AO, Félix FH, Leal LK, de Castro Brito GA, da Graça Naffah-Mazzacorati M, Viana GS. Valproic acid: an anticonvulsant drug with potent antinociceptive and anti-inflammatory properties. *Naunyn-Schmiedeberg's Arch Pharmacol*. 2013; 386(7): 575–587.
- [24] Lu WH, Wang CY, Chen PS, Wang JW, Chuang DM, Yang CS, Tzeng SF. Valproic acid attenuates microgliosis in injured spinal cord and purinergic P2X4 receptor expression in activated microglia. *J Neurosci Res*. 2013; 91(5): 694–705.
- [25] Thotala D, Karvas RM, Engelbach JA, Garbow JR, Hallahan AN, DeWees TA, Laszlo A, Hallahan DE. Valproic acid enhances the efficacy of radiation therapy by protecting normal hippocampal neurons and sensitizing malignant glioblastoma cells. *Oncotarget*. 2015; 6(33): 35004-35022.
- [26] Eckert M, Klumpp L, Huber SM. Cellular Effects of the Antiepileptic Drug Valproic Acid in Glioblastoma. *Cell Physiol Biochem*. 2017; 44(4): 1591-1605.
- [27] Vakilzadeh G, Khodaghali F, Ghadiri T, Darvishi M, Ghaemi A, Noorbakhsh F, Gorji A, Sharifzadeh M. Protective Effect of a cAMP Analogue on Behavioral Deficits and Neuropathological Changes in Cuprizone Model of Demyelination. *Mol Neurobiol*. 2015; 52(1): 130-141.
- [28] Ubogu E, Yosef N, Xia R, Sheikh K. Behavioral, electrophysiological, and histopathological characterization of a severe murine chronic demyelinating polyneuritis model. *J Peripher Nerv Syst*. 2012; 17(1): 53–61.
- [29] Boltze J, Kowalski I, Geiger K, Reich D, Gunther A, Buhrlé C, Egger D, Kamprad M, Emmrich F. Experimental treatment of stroke in spontaneously hypertensive rats by CD34+ and CD34- cord blood cells. *Ger Med Sci*. 2005; 3(Doc09), 1-13.
- [30] Carter R, Lione L, Humby T, Mangiarini L, Mahal A, Bates GP, Dunnett SB, Morton AJ. Characterization of Progressive Motor Deficits in Mice Transgenic for the Human Huntington's disease Mutation. *The Journal of Neuroscience*, April 15, 1999; 19(8): 3248–3257.
- [31] Grünblatt E, Bartl J, Iuhos D, Knezovic A, Trkulja V, Riederer P, Walitza S, Salkovic-Petrisic M. Characterization of cognitive deficits in spontaneously hypertensive rats, accompanied by brain insulin receptor dysfunction. *J Mol Psychiatry*. 2015; 3(1): 6.
- [32] Matsushima GK, Morell P. The neurotoxicant, cuprizone, as a model to study demyelination and remyelination in the central nervous system. *Brain Pathol*. 2001; 11(1): 107–116.
- [33] Sachs H, Bercury K, Popescu D, Narayanan S, Macklin W. A New Model of Cuprizone-Mediated Demyelination/Remyelination. *ASN Neuro*. 2014; 6(5): 1-16.
- [34] Yoshikawa K, Palumbo S, Toscano CD, Bosetti F. Inhibition of 5-lipoxygenase activity in mice during cuprizone-induced demyelination attenuates neuroinflammation, motor dysfunction and axonal damage. *Prostaglandins Leukot Essent Fat Acids*. 2011; 85(1): 43–52.
- [35] Koppel I, Timmusk T. Differential regulation of Bdnf expression in cortical neurons by class-selective histone deacetylase inhibitors. *Neuropharmacology*. 2013; 75: 106-115.
- [36] Boulle F, Hove D, Jakob SB, Rutten BP, Hamon M, van Os J, Lesch KP, Lanfumey L, Steinbusch HW, Kenis G. Epigenetic regulation of the BDNF gene: implications for psychiatric disorders. *Mol Psychiatry*. 2012; 17: 584-596.
- [37] Liu X, Zhu Z, Kalyani M, Janik J.M, Shi H. Effects of energy status and diet on Bdnf expression in the ventromedial hypothalamus of male and female rats. *Physiol. Behav*. 2014; 130: 99-107.
- [38] Liu X, Chopp M, Kassis H, Jia LF, Hozeska-Solgot A, Zhang RL, Chen C, Cui YS, Zhang ZG. Valproic acid increases white matter repair and neurogenesis after stroke. *Neuroscience*. 2012, 18; 220: 313–321.
- [39] Ye F, Chen Y, Hoang T, Montgomery RL, Zhao XH, Bu H, Hu T, Taketo MM, van Es JH, Clevers H, Hsieh J, Bassel-Duby R, Olson EN, Lu QR. HDAC1 and HDAC2 regulate oligodendrocyte differentiation by disrupting the beta-catenin-TCF interaction. *Nat Neurosci*. 2009; 12: 829–838.
- [40] Baumann N, Pham-Dinh D. Biology of oligodendrocyte and myelin in the mammalian central nervous system. *Physiol Rev*. 2001; 81: 871–927.
- [41] Brambilla R, Bracchi-Ricard V, Hu WH, Frydel B, Bramwell A, Karmally S, Green EJ, Bethea JR. Inhibition of astroglial nuclear factor  $\kappa$ B reduces inflammation and improves functional recovery after spinal cord injury. *J Exp Med* 2005; 202: 145–156.
- [42] Brambilla R, Hurtado A, Persaud T, Esham K, Pearse DD, Oudega M, Bethea JR. Transgenic inhibition of astroglial NF- $\kappa$ B leads to increased axonal sparing and sprouting following spinal cord injury. *J Neurochem*. 2009; 110: 765–778.

- [43] Taubert S, Gorrini C, Frank S, Parisi T, Fuchs M, Chan HM, Livingston DM, Amati B. E2F-Dependent Histone Acetylation and Recruitment of the Tip60 Acetyltransferase Complex to Chromatin in Late G1. *Mol Cell Biol.* 2004; 24(10): 4546–4556.
- [44] Shin YC, Choi KY, Kim WG. Cyclosporin A has a protective effect with induced upregulation of Hsp70 and nNOS on severe spinal cord ischemic injury in rabbits. *J Invest Surg.* 2007; 20: 113-120.
- [45] Faraco G, Pancani T, Formentini L, Mascagni P, Fossati G, Leoni F, Moroni F, Chiarugi A. Pharmacological inhibition of histone deacetylases by suberoylanilide hydroxamic acid specifically alters gene expression and reduces ischemic injury in the mouse brain. *Mol Pharmacol* 2006; 70: 1876-1884.